AFRL-VS-TR-2003-1565

ADVANCED MODELING OF THE IONOSPHERE AND UPPER ATMOSPHERE

Boris Khattatov

Environmental Research Technologies
1320 Pearl Street, Suite 108
Boulder, Colorado, 80302

1 May 2003

Scientific Report No. 1

AIR FORCE RESEARCH LABORATORY
Space Vehicles Directorate
29 Randolph Rd
AIR FORCE MATERIEL COMMAND
Hanscom AFB, MA 01731-3010

This technical report has been reviewed and is approved for publication.

/Signed/
JOHN RETTERER
Contract Manager

/Signed/
ROBERT MORRIS
Branch Chief

This document has been reviewed by the ESC Public Affairs Office and has been approved for release to the National Technical Information Service.

Qualified requestors may obtain additional copies form the Defense Technical Information Center (DTIC). All others should apply to the National Technical Information Service.

If your address has changed, if you with to be removed from the mailing list, or if the addressee is no longer employed by your organization, please notify AFRL/VSIM, 29 Randolph Rd., Hanscom AFB, MA 01731-3010. This will assist us in maintaining a current mailing list.

Do not return copies of this report unless contractual obligations or notices on a specific document require that it be returned.

REPORT DOCUMENTATION PAGE	*Form Approved* *OMB No. 0704-0188*

1. REPORT DATE *(DD-MM-YYYY)* 01-05-2003	**2. REPORT TYPE** Scientific Report No. 1	**3. DATES COVERED** *(From - To)* 10 Apr 00 - 1 Apr 03

4. TITLE AND SUBTITLE Advanced Modeling of the Ionosphere and Upper Atmosphere	**5a. CONTRACT NUMBER** F19628-02-C-0019
	5b. GRANT NUMBER
	5c. PROGRAM ELEMENT NUMBER
6. AUTHOR(S) Bori Khattatov	**5d. PROJECT NUMBER** 3005
	5e. TASK NUMBER SD
	5f. WORK UNIT NUMBER AC
7. PERFORMING ORGANIZATION NAME(S) AND ADDRESS(ES) Environmental Research Technologies 1320 Pearl Stree, Suite 108 Boulder, Colorado 80302	**8. PERFORMING ORGANIZATION REPORT NUMBER** ERT006i
9. SPONSORING/MONITORING AGENCY NAME(S) AND ADDRESS(ES) Air Force Research Laboratory (AFRL) 29 Randolph Road Bedford, MA 01731-3010 Contract Manager: John Retterer	**10. SPONSOR/MONITOR'S ACRONYM(S)**
	11. SPONSOR/MONITOR'S REPORT NUMBER(S) AFRL-VS-TR-2003-1565

12. DISTRIBUTION/AVAILABILITY STATEMENT

APPROVED FOR PUBLIC RELEASE; DISTRIBUTION UNLIMITED

13. SUPPLEMENTARY NOTES

14. ABSTRACT

Report developed under SBIR Contract AF Topic AF02-038. This interim report describes progress in developing a new numerical model of the ionosphere and related tangent-linear and adjoint models necessary for developing ionospheric data assimilation capabilities.

15. SUBJECT TERMS

SBIR Report, Ionosphere, Modeling, Electron content, Assimilation, GPS, HF, FAA

16. SECURITY CLASSIFICATION OF:			**17. LIMITATION OF ABSTRACT**	**18. NUMBER OF PAGES**	**19a. NAME OF RESPONSIBLE PERSON**
a. REPORT	**b. ABSTRACT**	**c. THIS PAGE**			John Retterer
U	U	U	SAR		**19b. TELEPHONE NUMBER** *(Include area code)* (781) 377-3891

Table of Contents

List of Figures

List of Tables

1. INTRODUCTION

Accurate knowledge of electron densities in the ionosphere is paramount for enabling precise navigation, uninterrupted ground-to-satellite communications, high accuracy positioning, and surveillance. Thus, an ability to forecast regional ionospheric conditions has applications in most areas of military operations, from HF communications to delivering vital data to individual soldiers in remote battlefields, to precision-guided weapons, to space based intelligence gathering and space object tracking.

During the first year of the AF sponsored SBIR Phase II investigation we developed a new computer model for simulating time evolution of ion and electron densities in the ionosphere on a global scale and developed the corresponding tangent linear and adjoint models with respect to parallel transport.

These new computational tools will further evolve into a prototype numerical ionospheric forecast systems, that will assimilate available measurements of ionospheric electron content from networks of ground-based GPS reference stations and other instruments.

Significant improvements in the reliability of conventional weather forecasts in the last decade or so are largely due to advances in data assimilation techniques. The atmosphere, including the ionosphere, is a chaotic system; small errors in the initial conditions of a forecast grow rapidly, and affect predictability. Furthermore, predictability is limited by model errors due to the approximate simulation of relevant physical processes in the numerical models and to a poorly known external forcing. Data assimilation aims to decrease these uncertainties by using observations to obtain better initial conditions and/or to provide better estimates of poorly known empirical quantities in parameterizations of various physical processes in the models.

Development of practical and efficient data assimilation schemes as well as operational implementations of forecast systems depend critically on the design, quality, and maintainability of the underlying physical propagator model.

In the course of the Phase I investigation it was decided that the computer code of the model available to us, Coupled Thermosphere Ionosphere Model (CTIM), is unacceptable for the purpose of adding on data assimilation capabilities and practical implementation of the forecast system for several reasons, with major reasons listed below:

- Very poor quality of code leading to inefficiencies, redundancy, and making code hard to understand and modify.
- Almost complete lack of documentation.
- Extensive use of Fortran 77 and Fortran 66 features that are being phased out in the modern and future compiler versions.

The first major task of the Phase II investigation was then creating a new computer code implementing the model and performing the first round of validation. This task is largely completed, certain features of the model that are deemed as non-critical are still left in the development stage (.e.g., correct calculations of night time ionization rates; high-latitude transport) and will be added after testing the model and assimilation scheme with real GPS data.

While development of the propagator model "from scratch" took time, we deem it to be an absolutely crucial component that will enable and strongly facilitate reaching the end objective. For example, building the tangent linear and adjoint models that are necessary for implementing data assimilation capabilities for existing numerical global atmospheric models usually take several person-years. In this Phase II effort the development of both components with respect to parallel transport took less than 2 person-days.

We believe that these reductions in the development time are due to adherence to modern software development practices and tools, object-oriented programming style, and maintaining well-documented code throughout the duration of the project.

The following personnel contributed to the development of the model: Dr. Boris Khattatov, PI; Dr. Michael Murphy, Senior Computer Scientist; Mr. James Adams, Senior Software Engineer; Dr Timothy Fuller-Rowell, Consultant.

2. MODEL

The developed model is a numerical global model of the ionosphere system loosely based on Millward et al (1996), Bailey and Balan (1996), Fuller-Rowell (1996) and Huba et al (2000).

The dynamic equations and vertical ExB transport for seven ions (H, O, O_2, He, NO, N_2, N) are solved on a fixed Eulerian grid in magnetic p, q, and longitude coordinates. An example of the low-latitude configuration is shown below (only 20 longitudes and 30 p values are shown for clarity, regular model configuration is 100x100x100).

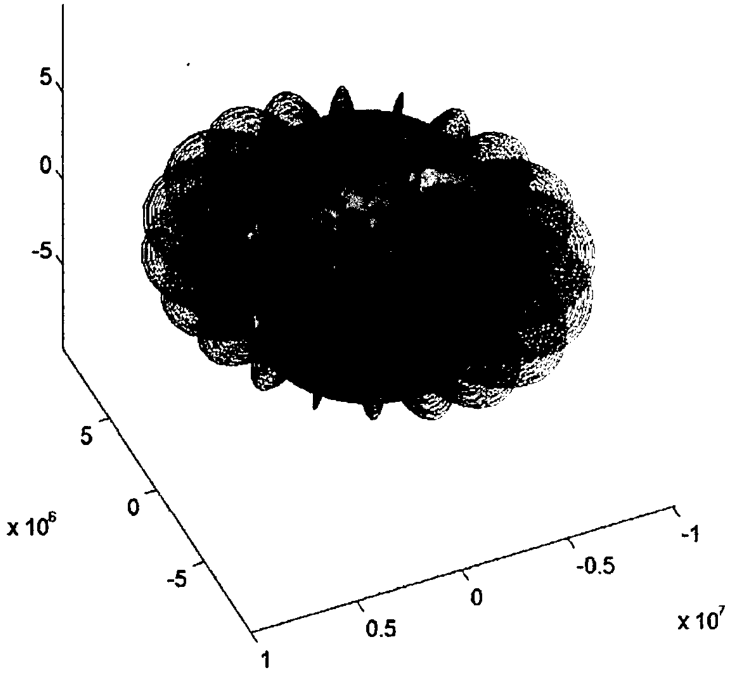

Figure 1. A part of the model magnetic grid.

The model solves plasma dynamics equations -- parallel and ExB continuity and momentum -- for seven ion species and electrons and energy conservation equation for the three major ions and electrons. The model includes chemical interactions with neutrals and ion-ion and ion-neutral collision rates and Photoionization. ExB drift is computed by via Fejer&Scherless model at the equator and by Weimer (2000) model at high latitude. The high-latitude transport is currently turned-off pending model validation at low latitudes.

Model prognostic, external and diagnostic variables are listed in Tables 1-3.

Variable Name	Units	Description	Comments
Ion densities	particles/ m^3	Local (point) volume density of a particular ion species	at present there are 7 ions: O^1, H^1, He^1, N_2^1, O_2^1, NO^1, N^1
Ion temperatures	K, degree	Local temperature of a particular ion species	same
Ion velocities	m/s	Local (point) velocity of a particular ion species along the magnetic field line passing through this point	same
Electron temperature	K, degree	Local electron temperature	
Electron velocity	m/s	Local (point) velocity of electrons along the magnetic field line passing through this point	
Electron density	particles/ m^3	Local (point) volume density of electrons	is the sum of all local ion densities

Table 1. Model Prognostic Variables

Variable Name	Units	Description	Comments
Neutral densities	particles/ m^3	Local (point) volume density of a particular neutral species	- at present there are 7 neutrals: O, O_2, N_2, He, H, NO, N.
Neutral temperature	K, degree	Local temperature of all neutral species (one for all)	same
Neutral zonal velocity	m/s	Local (point) velocity of all neutral species (one for all) in the zonal direction (east-west, eastward is positive)	same
Neutral meridional velocity	m/s	Local (point) velocity of all neutral species (one for all) in the meridional direction (north-south, northward is positive)	same

Table 2. Model External Variables

Variable Name	**Units**	**Description**	**Comments**
ExB zonal velocity	m/s	Local (point) velocity associated with the zonal ExB drift of the magnetic field line passing through this point	Needs to be computed from empirical ExB models
ExB meridional velocity	m/s	Local (point) velocity associated with the meridional ExB drift of the magnetic field line passing through this point	same as above
Photo production	Particles/s/m^3	Number of particles of a particular ion species produced as a result of photoionization per second per unit volume.	- at present there are 7 neutrals, only 5 of those can be photoionized: O, O_2, N_2, He, N. Other ions are produced via chemical reactions, such as $O^+ + H \rightarrow H^+ + O$.
Chemical production	Particles/s/m^3	Number of particles of a particular ion species produced as a result of chemical reactions per second per unit volume.	There are 21 chemical reactions at the present. e.g., $O^+ + H \rightarrow H^+ + O$.
Chemical loss	Particles/s/m^3	Number of particles of a particular ion species lost as a result of chemical and recombination reactions per second per unit volume	This value is a product of the density (concentration) of the ion species being destructed and the *chemical loss rate, L.*
Photoionization rates	1/s	Coefficients needed to compute photo production	- at present there are 7 neutrals, only 5 of those can be photo-ionized: O, O_2, N_2, He, N.
Chemical reaction rates	m^3/s	Coefficients needed to compute chemical loss due to electron exchange reactions.	There are 21 chemical reactions at the present. e.g., $O^+ + H \rightarrow H^+ + O$.
Recombination reaction rates	1/s	Coefficients needed to compute loss due to recombination chemical reactions	There are 7 recombination reactions, e.g., $O^+ + e \rightarrow O$. e represents an electron.
Ion-neutral collision frequencies	1/s	Drag on a particular ion particle due to collisions with a neutral species.	There are 7 ions and 7 neutrals, therefore it is a 7x7 matrix with zero diagonal.
Ion-ion collision frequencies	1/s	Drag on a particular ion particle due to collisions with a different ion species.	There are 7 ions, therefore it is a 7x7 matrix with zero diagonal.
Ion heating rates	J/m^3/s	Heating due to Joule heating, frictional collisions and other processes.	Is only computed for three major ions, O^+, H^+, He^+
Ion thermal conductivities	J/K/m/s		Is only computed for three major ions, O^+, H^+, He^+
Electron heating rates	J/m^3/s	Heating due to Joule heating, frictional collisions and other processes.	
Electron thermal conductivities	J/K/m/s		

Table 3. Model Diagnostic Variables

2.1 Prognostic Equations

A prognostic equation allows one to estimate a particular prognostic variable at a future time. The prognostic variables are density, velocity and temperature for ions and electron density, temperature and velocity.

These equations are given in dipole coordinates, along magnetic flow tubes. Therefore there is only one dependent spatial coordinate corresponding to the position along the magnetic flow tube. This can be a non-dimensional variable q or a dimensional variable $s = q \cdot \mathrm{R_c}$ (Re is the radius of the earth),

2.1.1 Continuity Equation For Each Ion Species

Numerical solution of this equation should generate ion density $N_i(t + \Box t)$ given all related variables at time *t*.

$$\frac{\partial N_i}{\partial t} - b_s^2 \frac{\partial\left(\frac{N_i V_i}{b_s}\right)}{\partial s} + N_i \cdot \nabla V_\perp + \nabla N_i \cdot V_\perp = P_i - L_i \cdot N_i \tag{1}$$

where

N_i – density of ion i

V_i – velocity (aligned with the magnetic flow tube) of ion i

$s = q \cdot \mathrm{R_c}$

$b_s = \sqrt{1 + 3\cos^2(eccLat)} \cdot \left(\frac{\mathrm{R_e}}{eccRadius}\right)^3$

P_i – chemical production + photochemical production

L_i – chemical loss rate

$L_i \cdot N_i$ – chemical loss

The term

$$\nabla V_\perp = \frac{6 \cdot V_\perp^{eq} \sin^2(eccLat) \cdot (1 + \cos^2(eccLat))}{p \cdot R_e \cdot (1 + 3 \cdot \cos^2(eccLat))^2} \tag{2}$$

is a divergence of ExB velocity in the vertical (and meridional) plane, i.e., in p direction. $V_\perp^{eq}$ is the value of ExB meridional drift at the magnetic equator corresponding to a particular p.

2.1.2 Momentum Equation For Each Ion Species

Numerical solution of this equation should generate ion velocity $V_i(t + \Box t)$ given all related variables at time *t*.

$$V_i = \frac{1}{\sum\limits_{n=1}^{N\_Neutrals} \nu_{in} + \sum\limits_{j=1}^{N\_Ions} \nu_{ij}} \cdot \left[\begin{array}{l} -g \sin I + \frac{b_s k_i}{m_i}\left(\frac{T_i}{N_i}\frac{\partial N_i}{\partial s} + \frac{T_e}{N_e}\frac{\partial N_e}{\partial s} + \frac{\partial(T_i + T_e)}{\partial s}\right) \\ + \sum\limits_{n=1}^{N\_Neutrals} \nu_{in}(V_n \cos D - U_n \sin D)\cos I + \sum\limits_{j=1}^{N\_Ions} \nu_{ij} V_j \end{array} \right] \tag{3}$$

where

N_i – density of ion i

V_i – velocity (aligned with the magnetic flow tube) of ion i

V_j – velocity of ion j.

$s = q \cdot \mathrm{R_c}$

$b_s = \sqrt{1+3\cos^2(eccLat)} \cdot \left(\dfrac{\mathrm{R_c}}{eccRadius}\right)^3$

m_i – mass of ion i.

k – Boltzmann's constant.

T_i – temperature of ion i.

T_e – electron temperature

N_e – electron density.

U_n – zonal neutral velocity.

V_n – meridional neutral velocity.

ν_{in} - ion-neutral collision frequency.

ν_{ij} - ion-ion collision frequency.

g – acceleration of gravity.

I – inclination angle for this flow tube:

$\sin I = \dfrac{2\cos(eccLat)}{\sqrt{1+3\cos^2(eccLat)}}$

$\cos I = \dfrac{\sin(eccLat)}{\sqrt{1+3\cos^2(eccLat)}}$

D – declination angle for this flow tube.

2.1.3 Energy Equation For Each Ion Species

Numerical solution of this equation should generate ion temperature $T_i(t+\square t)$ given all related variables at time *t*.

$$\frac{3}{2}kN_i\left(\frac{\partial T_i}{\partial t}+V_\perp \nabla T_i\right)=kN_iT_ib_s^2\frac{\partial}{\partial s}\left(\frac{V_i}{b_s}\right)-kN_iT_i\cdot\nabla V_\perp+b_s^2\frac{\partial}{\partial s}\left(\kappa\frac{\partial T_i}{\partial s}\right)+\frac{3}{2}kN_iV_ib_s\frac{\partial T_i}{\partial s}+Q+F \qquad (4)$$

Where

Q and F - are the heating rates

κ - is the thermal conductivity

2.1.4 Electron Temperature Equation

It is similar to ion temperature equation, except that the conductivities and heating rates are computed for electrons.

2.1.5 Electron Density Equation

$$N_e = \sum_{i=1}^{NumberOfIons} N_i \tag{5}$$

2.1.6 Electron Velocity Equation

Assumes that there are no field-aligned currents:

$$V_e = \frac{\sum_{i=1}^{NumberOfIons} V_i N_i}{N_e} \tag{6}$$

2.2 Timing

On a Pentium Xeon 2.2GHz computer, 1 model time step requires 35 seconds in a configuration with 10^6 grid points and the memory footprint is 1.5 Gb.

3. SELECTED RESULTS

In this section we will present selected results obtained from different numerical experiments.

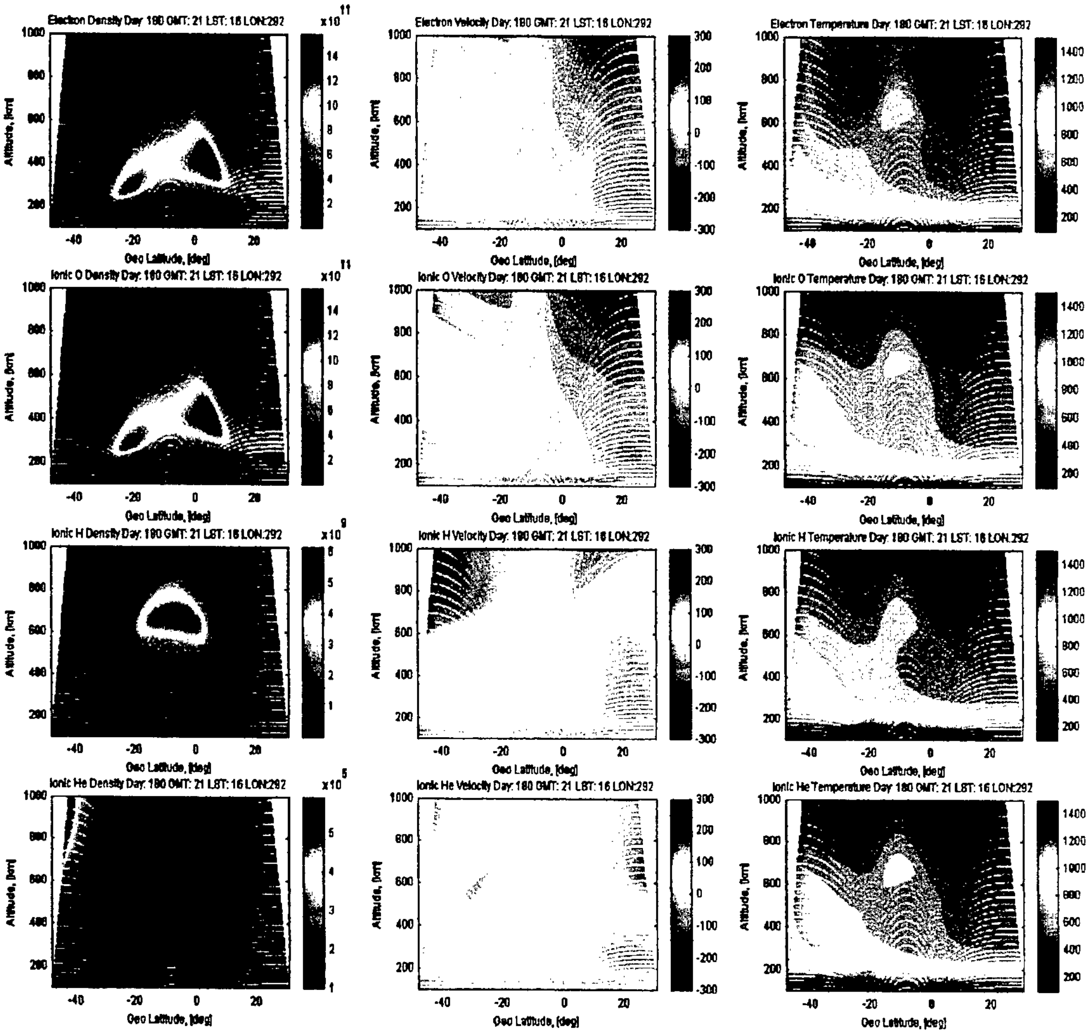

Figure 2. Examples of instantaneous model prognostic variables for electrons and major ions shown as q-p cross sections at a fixed magnetic longitude.

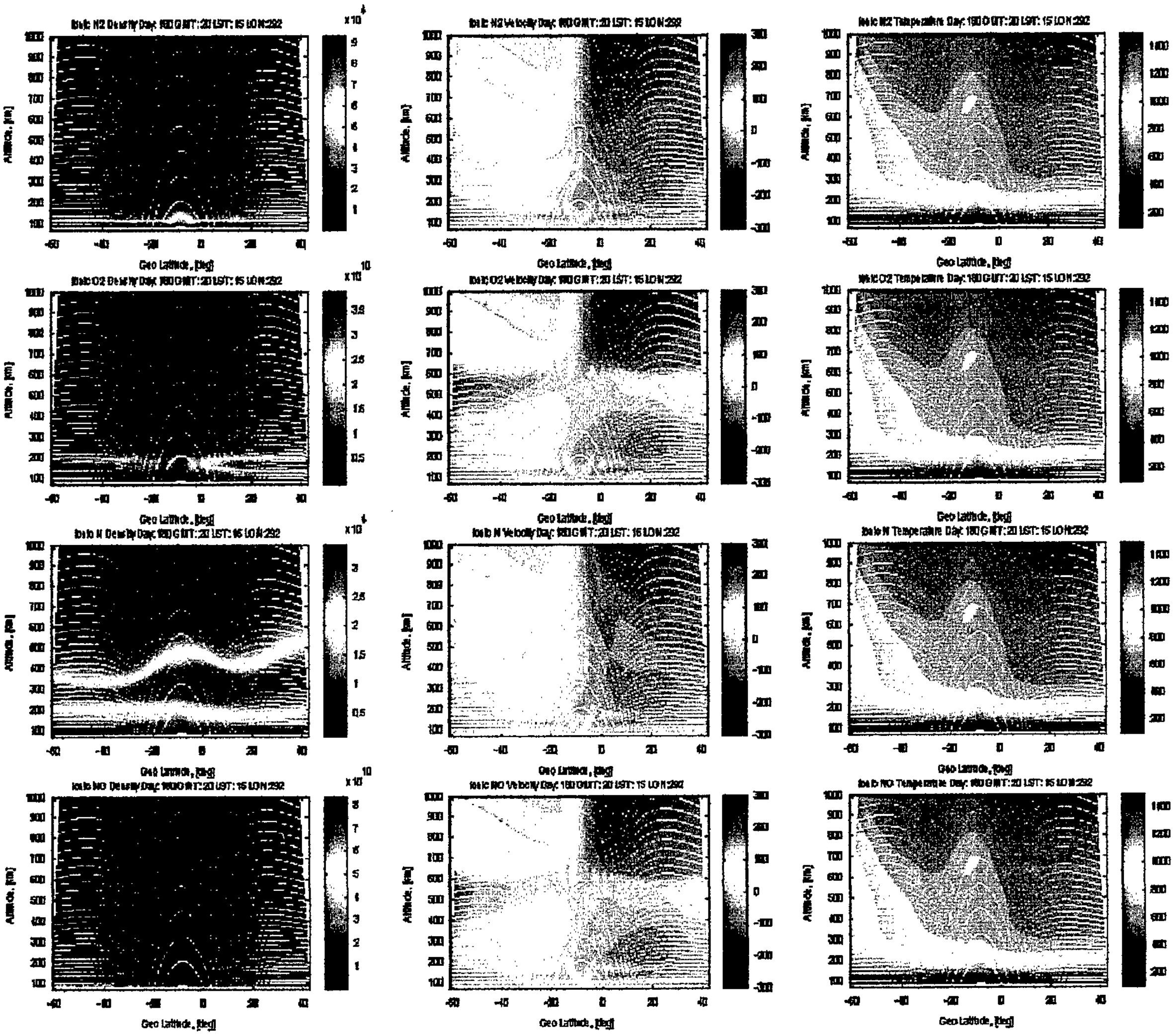

Figure 3. Examples of instantaneous model prognostic variables for minor ions shown as q-p cross sections at a fixed magnetic longitude.

Figure 4. An example of 3-D instantaneous iso-surface of constant electron density. The radial direction is exaggerated to show detail.

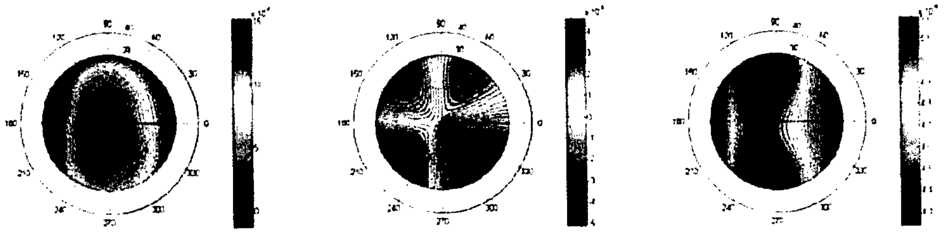

Figure 5. The x, y, and z-components of the Earth's magnetic field at the North Pole

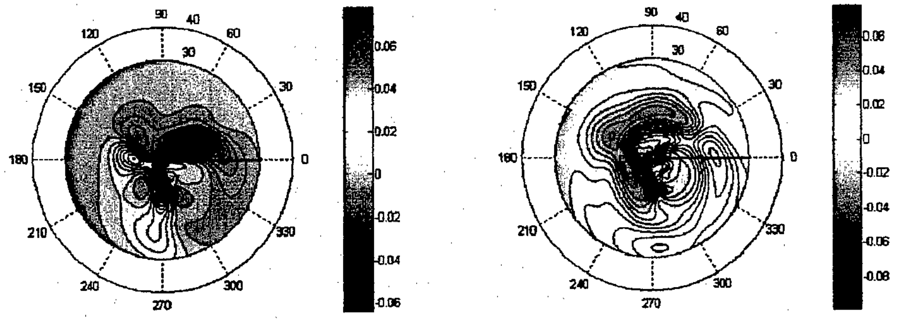

Figure 6. The x- and y-component of the Weimer electric potential at the North Pole.

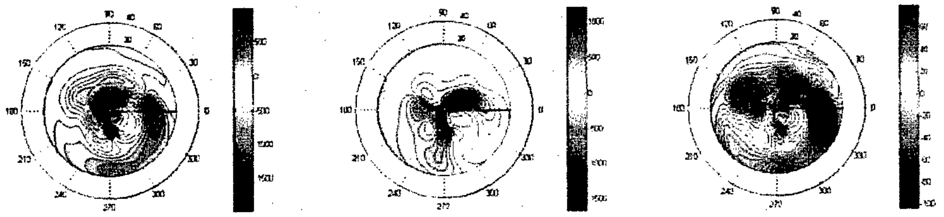

Figure 7. Calculated x-, y-, and z- component of the ExB drift velocities near the North Pole.

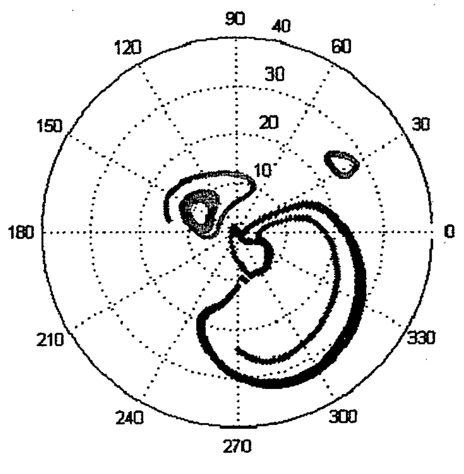

Figure 8. Trajectories of particles in the magnetic field acting under ExB drift with different starting locations near the Noth Pole.

4. TANGENT LINEAR AND ADJOINT MODELS

In the case of the ionosphere, lets assume that the model **M** is a forward time-dependent discrete propagator that accepts the current state $\mathbf{x}_t$ (electron or ion densities throughout the model domain arranged in a vector) and values of several atmospheric drivers $\mathbf{p}_t$ (e.g., level of solar activity, etc) as inputs and generates state estimates for a later time:

$$\mathbf{x}_{t+\Delta t} = \mathbf{M}(\mathbf{p}_t, \mathbf{x}_t) \tag{7}$$

Both quantities, $\mathbf{x}_t$ and $\mathbf{p}_t$, are considered to be model parameters.

Generally speaking, the tangent linear of the model M is simply a derivative of the results with respect to the initial conditions or input parameters. Note that **M** is a non-linear vector function and therefore its linearizations (first derivatives) are matrices:

$$\mathbf{L}_{\mathbf{x}} = \frac{\partial \mathbf{M}}{\partial \mathbf{x}} \text{ and } \mathbf{L}_{\mathbf{p}} = \frac{\partial \mathbf{M}}{\partial \mathbf{p}} \tag{8}$$

The adjoint of the propagator model is simply a transposed of the matrix L or, a way to compute a product of the transposed and an arbitrary vector. The linearization matrix describes sensitivity of the model with respect to the initial conditions and the adjoint is used to either minimize the cost function in the variational assimilation approach or to solve the Kalman filter equations. Both these matrices are fundamental to implementing data assimilation schemes.

These linearization matrices can be obtained in several ways:

- approximated via finite-differences calculations, i.e., by introducing small changes in $\mathbf{x}_t$ and/or $\mathbf{p}_t$ and computing resulting changes in $\mathbf{x}_{t+\Delta t}$:

$$\mathbf{L}_{\mathbf{x}} \approx \frac{\Delta \mathbf{M}}{\Delta \mathbf{x}_t} = \frac{\Delta \mathbf{x}_{t+\Delta t}}{\Delta \mathbf{x}_t} \tag{9}$$

- by differentiating the actual computer code (e.g., Fortran or C) implementing the model and generating computer code for direct computation of **L**.

- by analytical differentiation of theoretical equations of the model and coding the results.

The first approach can be extremely CPU intensive but is straightforward to implement. The other two are much more efficient but can be hard to implement and will have to be re-done if changes are introduced into the model.

We followed a variation of the second approach and obtained and coded explicit calculations of both these matrices for each plasma tube in the model. An example of the linearization matrix is shown in Figure 9 for O^+.

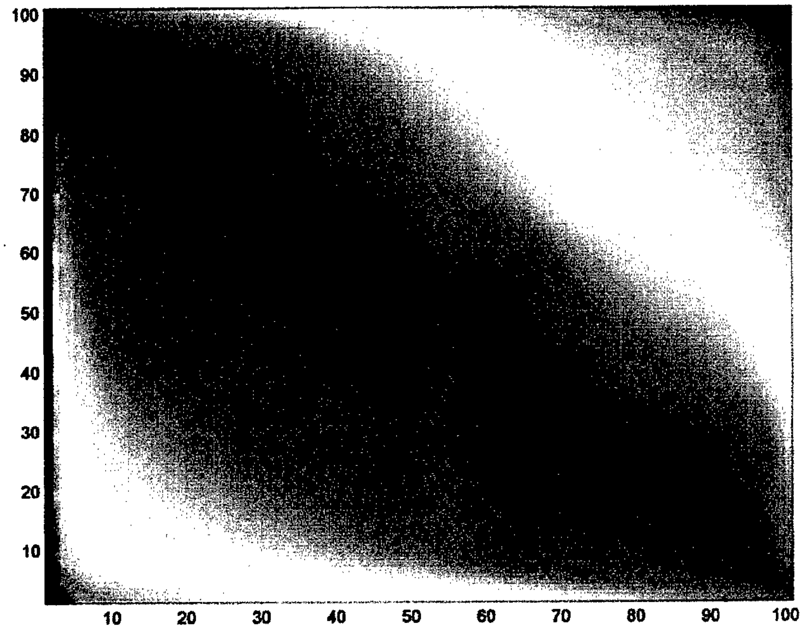

Figure 9. An example of logarithm of absolute value of linearization matrix for one plasma tube.

The particular plasma tube has 100 points and changes in ion densities at the next time step can be obtained by multiplying this matrix by a vector of changes in ion density for this tube at a previous tie step. The asymmetries in the matrix reflect the fact that in this particular case the prevailing parallel transport is directed from the top-left end of the tube to the bottom-right.

Once the linearization matrix is obtained, evolution of the error-covariance matrices for different points on the same tube can be trivially computed as follows (Khattatov et al., 1999):

$$\mathbf{C}(t+\Delta t) = \mathbf{L}_{\mathrm{x}}\mathbf{C}(t)\mathbf{L}_{\mathrm{x}}^{T}$$

5. CONCLUSIONS

The initial Phase II development effort led to creation of a new ionospheric numerical global model by its design particularly well suited for use with a data assimilation scheme. The corresponding linear and adjoint model with respect to parallel transport were implemented and are ready for experiments with real data. In the remaining 12 months of this investigation we plan to implement a prototype system for now-casting and forecasting three-dimensional global electron densities in the ionosphere constrained by a sequential data assimilation scheme and validate the system performance.

REFERENCES

Millward et al.,1996, A coupled thermosphere-ionosphere-plasmosphere model (CTIP), in *STEP: Handbook of Ionospheric Models*, STEP Report, editor R.W. Schun.

Bailey and Balan, 1996, A low-latitude ionosphere-plasmosphere model, in *STEP: Handbook of Ionospheric Models*, STEP Report, editor R.W. Schunk.

Huba et al., 2000, SAMI2 is another model of the ionosphere: a new low-latitude ionosphere model, *J. Geophys. Res.*, 23,035.

Fuller-Rowell T.J., D. Rees, S. Quegan, R.J. Moffett, M.V. Codrescu, and G.H. Millward, 1996, A coupled thermosphere ionosphere model (CTIM). *Handbook of Ionospheric Models*, STEP Report, editor R.W. Schunk.

Khattatov, B. V., J. C. Gille, L. V. Lyjak, G. P. Brasseur, V. L. Dvortsov, A. E. Roche, and J. Waters, 1999, Assimilation of photochemically active species and a case analysis of UARS data., *J. Geophys. Res., 104,* 18,715-18,737.